

Gear-Meshed Tiling of Surfaces with Molecular Pentagonal Stars

Quirin Stöckl,[†] Davide Bandera,[‡] Craig S. Kaplan,[§] Karl-Heinz Ernst,^{*,†,‡} and Jay S. Siegel^{*,†,‡,¶}

[†]Empa, Swiss Federal Laboratories for Materials Science and Technology, 8600 Dübendorf, Switzerland

[‡]Department of Chemistry, University of Zurich, 8057 Zürich, Switzerland

[¶]School of Pharmaceutical Science and Technology, Tianjin University, 92 Weijin Road (A203/Bldg 24), Nankai District, Tianjin 300072, PR China

[§]University of Waterloo, Waterloo N2L 3G1, Ontario, Canada

Supporting Information

ABSTRACT: The assembly of the chiral pentagonal-star-shaped 1,3,5,7,9-pentaphenylcorannulene on a Cu(111) surface has been studied with scanning tunneling microscopy. Two different long-range ordered phases coexist at 60 K, most likely racemic and homochiral phases. The principal motifs emulate a network of meshed gears. One of the observed structures resembles the densest packing of five-fold symmetric stars.

Five-fold-symmetry is common in organisms and molecules but is incompatible with the translational order of a classical crystal lattice or planar tiling.¹ As such, tilings with pentagons are nontrivial. None of the 17 plane groups representing periodic tessellations of the Euclidian plane display five-fold-symmetry.² Employing inhomogeneous tiling types, Kepler, Dürer, and Penrose proposed plane-filling solutions by considering rigid pentagons and stars.^{3,4} Such patterns can also be observed in the Islamic tessellations,⁵ but all solutions result in aperiodicity or lower symmetry.⁶

Given these symmetry restrictions, it may be misconstrued that pentacles cannot or do not crystallize—but they do! Despite speculations that supercooled liquids and metallic glasses possess icosahedral short-range order,^{7,8} which might be also important structures for glass transition and melting processes,⁹ pentagonally symmetric molecules do freeze into crystals and adopt regular arrangements on surfaces with a prerequisite loss of symmetry, the highest molecular site symmetry being C_5 .

Empirical/phenomenological solutions have played an important role for understanding how convex pentagons tile. Pentagonal star-shaped tiles (i.e., concave decagons) offer an added complication due to their inherent ability to interdigitate, but also here engineering solutions provide insight.¹⁰ Reasoning by analogy leads one to the parallel between stars and gears.¹¹ When gears mesh, there are preferred conformations (locally C_2 and C_5 symmetric). In the densest pattern for pentagonal stars, nearest neighbor conformations along perpendicular lines adopt such C_5 and C_2 conformations, resulting in an overall unit cell symmetry of $p2mg$.

Fragment bowls of buckminsterfullerene (C_{60}), first of all corannulenes ($C_{20}H_{10}$, **1**, Figure 1), possess five-fold symmetry axes. Buckybowls based on chiral 1,3,5,7,9-pentastituted derivatives of **1** offer, therefore, a unique opportunity to

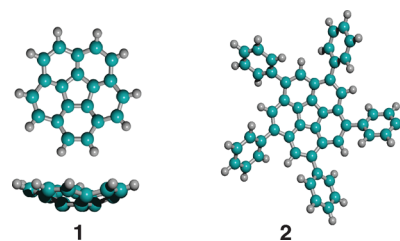


Figure 1. Ball-and-stick molecular models of corannulene (**1**) and pentaphenylcorannulene (**2**).

investigate close-packing strategies of five-fold-symmetric molecular stars on surfaces. In particular, the chemistry that has been developed for these bowl-shaped polynuclear aromatic hydrocarbons^{12,13} bodes well for comparison of different pentagonal shapes.

Assembly of five-fold-symmetric, shape-persistent macrocycles has been previously studied at the solid–liquid interface,^{14,15} and pentagonal features were discussed for rubrene and para-terphenyldicyano cerium on noble metal surfaces;^{16,17} however, systematic studies of close-packing strategies of pentagonal molecules in the plane have only been addressed with pentasubstituted derivatives of **1** so far.^{18–20} Besides the motivation to understand packing strategies of five-fold-symmetric molecules in the plane, modification of metal surfaces with **1** and its derivatives was performed with the goal to study symmetry-mismatch between surface and molecules,²¹ bicomponent packing,²² two-dimensional (2D) phase transitions,^{23,24} and surface-induced ball- and bowl-in-bowl complexation^{25,26} and to understand the origin of interface dipole moments without charge transfer.²⁷

Adsorbed on Cu(111) **1** circumvents C_5 symmetry by manifesting a geometry with one hexagonal ring oriented parallel to the surface.²³ Pentachloro- and pentamethylcorannulene maintain the C_5 axis of the bowl normal to the surface,^{18,20} and display 2D packing motifs essentially identical with that of rigid pentagon packing.^{28,31}

Scanning tunneling microscopy (STM) of close packed pentagonal star-shaped 1,3,5,7,9-penta-phenylcorannulene ($C_{50}H_{30}$, **2**) on a copper(111) surface was performed under ultrahigh vacuum ($p < 2 \times 10^{-10}$ mbar) conditions. A complete

Received: November 5, 2013

Published: December 27, 2013

monolayer of **2** was deposited onto a Cu(111) single crystal surface, held at room temperature (RT), by evaporation from a Knudsen cell held at 460 K for 30 min. The 2D crystal phases were observed at room temperature, but STM was performed at 60 K (LT) for better resolution and minimizing thermal drift. The analyses of the STM images are described in the Supporting Information (SI).

Two different coexisting structures were identified in the STM images (Figure 2). The periodicity of the adsorbate

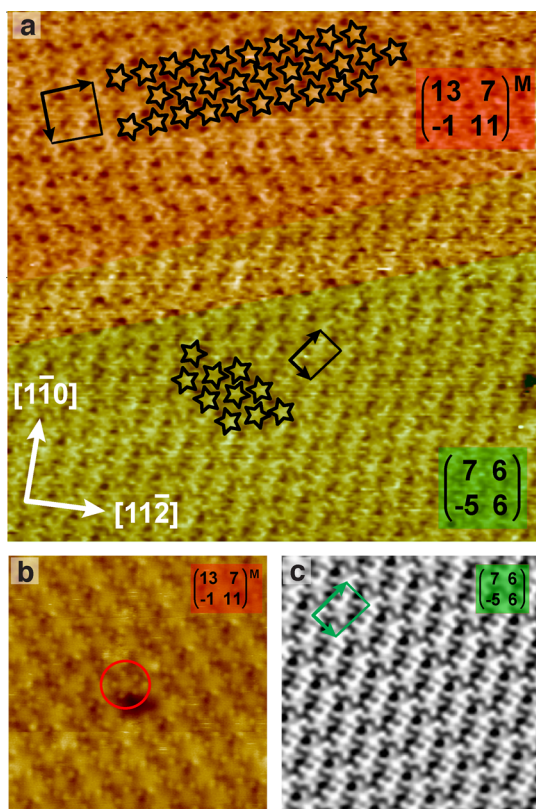


Figure 2. STM images of **2** at monolayer saturation coverage. (a) The long-range scan reveals two coexisting phases (55 nm × 55 nm, $U = 857$ mV, $I = 56$ pA, RT) with $(13\ 7, -1\ 11)^M$ and $(7\ 6, -5\ 6)$ unit cell periodicities. Stars are superimposed on some molecules in order to highlight the packing motifs. (b) STM image of the $(13\ 7, -1\ 11)^M$ phase (14.29 nm × 14.29 nm, $U = 743$ mV, $I = 25$ pA, LT). For a molecule near a defect, all five phenyl rings are clearly identified. (c) Averaged STM image of a $(7\ 6, -5\ 6)$ domain. (13 nm × 13 nm, $U = 857$ mV, $I = 56$ pA, LT, image averaged over 200 positions (see SI).

lattices with respect to the Cu(111) substrate was determined as $(13\ 7, -1\ 11)^M$ and $(7\ 6, -5\ 6)$,^{32,33} with packing densities of 36.5 and 36 Cu surface atoms per molecule, respectively. In both structures, single molecules appear clearly as five-fold symmetric stars with the phenyl groups representing the points. Previous adsorption studies of corannulenes found the convex face always turned toward the surface.^{18–24} Dark central spots suggest the same orientation for **2** (Figure S1, SI). As found for **1** by theoretical means, the high π -electron density causes a Pauli repulsion of substrate electrons and creates a strong electrostatic bond.³⁴

The adsorption energy of molecules at surfaces favors 2D close-packing (i.e., highest density). Both structures observed here have almost identical density. The $(7\ 6, -5\ 6)$ phase has a typical chevron-pattern, with every second row in an

antiparallel orientation (Figure 3a). This motif has been identified as the densest packing for rigid pentagons in the

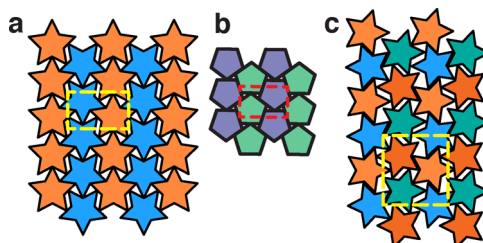


Figure 3. Close packing of pentagonal stars and pentagons. The plane symmetry groups are p2mg (a,b) and p2gg (c). The rectangular unit cells are indicated.

Euclidean plane (Figure 3b),³⁵ covering 92.1% of the entire area. The specific packing fraction for stars depends on the opening angle between the points, ranging from 0.921 for 180° (pentagons) to basically zero for 72° (stick figure). However, it is conjectured here that the analog tiling with antiparallel rows of stars represents the densest packing for a given star type (Figure S2, SI).¹⁰ Similar to the dense-packing problem of stars are hard cyclic pentamers, constructed from five circular disks. A striped phase was there identified via Monte Carlo simulations as well.^{36–38} Due to the possibility of interdigitation, the packing fraction for such cyclic pentamers can become slightly higher than those found for regular pentagons.

The second packing has four molecules per unit cell. Not only do adjacent rows have different star orientations, but also within a row only every second star is identically oriented. The points follow a zigzag motif, with a second glide plane but no mirror plane. The packing density is only slightly higher, thus correlating equal density with packing motif coexistence in the monolayer. Judged by long-range STM images, both phases cover equal area (50:50 ± 3%). Phase boundaries coincide often with substrate steps, but when on flat terraces they are very narrow; geared molecules only reorient (Figure S3, SI).

Another reason for the occurrence of different structures might be that the monolayer is built up by chiral molecules. Therefore, one phase could be a racemate crystal, while the other constitutes a conglomerate of homochiral domains (Figure 4).^{39,40} Both phases break the mirror symmetry of the underlying substrate; i.e., mirror domains are observed (Figure S4, SI). The STM results do not allow conclusions about hetero- or homochirality of the structures. The $(13\ 7, -1\ 11)^M$ phase is arbitrarily chosen to be heterochiral (Figure 4a), and the $(7\ 6, -5\ 6)$ phase to be homochiral (Figure 4b). Similar packing densities are achieved with the opposite hetero/homochiral content (Figure S5, SI).

In all models the edges of the phenyl rings point roughly perpendicular to the plane of a phenyl ring of an adjacent molecule. Such a T-shape interaction has been observed in 2D structures of tetraphenyl porphyrins on surfaces.⁴¹

The fact that clustering but not ordering is seen at low coverage points to weak attractive interactions among molecules of **2** (Figure S6, SI). Consequently, the ordered structures (Figure 2) are a result of the dense packing of **2** at monolayer saturation coverage. These dense 2D crystal phases of **2** on a copper(111) surface can be well modeled by tiling the plane with gear-meshed pentagonal stars. The two observed packing patterns correspond to those of highest density, but diastereomeric packings could not be excluded.

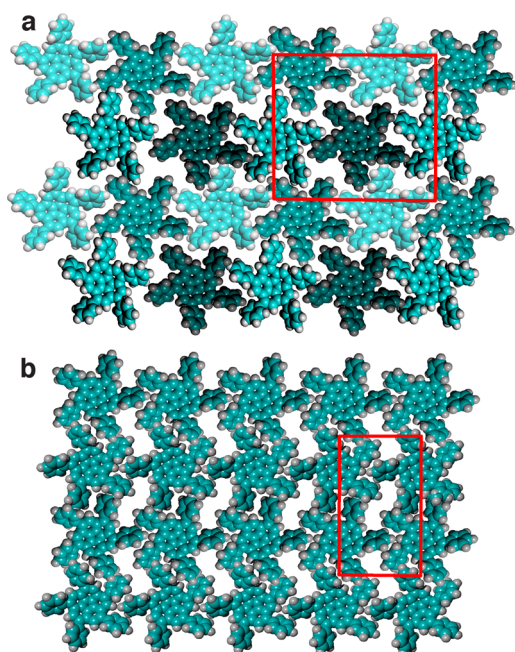


Figure 4. Model structures for the two observed phases with heterochiral and homochiral content. (a) $(13\ 7, -1\ 11)^M$, different handedness and orientations are indicated by different color tones. (b) Homochiral $(7\ 6, -5\ 6)$ phase. Unit cells are indicated as red rectangles. For other models, see: Figures S4 and S5 in SI.

■ ASSOCIATED CONTENT

📄 Supporting Information

STM acquisition and analysis procedures, STM images, densest pentagonal star tiling, homo- and heterochiral model structures (Figures S1–S6). This material is available free of charge via the Internet at <http://pubs.acs.org>.

■ AUTHOR INFORMATION

Corresponding Authors

dean_spst@tju.edu.cn

karl-heinz.ernst@empa.ch

Notes

The authors declare no competing financial interest.

■ ACKNOWLEDGMENTS

Financial support by the Swiss National Science Foundation (SNSF)—project FUNDASA—and Collaborative Innovation Center of Chemical Science and Engineering (Tianjin) is gratefully acknowledged. We thank Hans-Beat Bürgi for fruitful discussions.

■ REFERENCES

- (1) Buerger, M. J. *Elementary Crystallography: An Introduction to the Fundamental Geometrical Features of Crystals*; Wiley: New York, 1956.
- (2) Cracknell, A. P. *Thin Solid Films* **1974**, *21*, 107–127.
- (3) Lück, R. *Mater. Sci. Eng., A* **2000**, *294–296*, 263–267 and references therein.
- (4) Caspar, D. L. D.; Fontano, E. *Proc. Natl. Acad. Sci. U.S.A.* **1996**, *93*, 14271–14278 and references therein.
- (5) Lu, P. J.; Steinhardt, P. J. *Science* **2007**, *315*, 1106–1110.
- (6) Hargittai, I., Ed. *Fivefold Symmetry*; World Scientific: Singapore, 1992.
- (7) Frank, F. C. *Proc. R. Soc., London, Ser. A* **1952**, *215*, 43–46.
- (8) Hoare, M. R. *Adv. Chem. Phys.* **1979**, *40*, 49–135.
- (9) D., R. *Phys. Rev. B.* **1983**, *28*, 5515–5535.

(10) The goal to cut a set of five-pointed stars from a sheet of acrylic using a laser cutter led C.S.K. to make the packing as dense as possible so as to maximize the number of stars that could be obtained for a fixed sheet area, with a secondary goal to make the cutting process as efficient as possible (i.e. minimizing the total distance travelled by the laser head). A natural starting point in the search for a dense packing motif is to consider arrangements in which a star's convex point coincides with the reflex angle of an adjacent star, thereby consuming some of the area of the triangular dents between both stars' points. By rotating the stars so that two edges coincide, the laser can cut these two edges simultaneously, thus shortening the total tool path. Trial and error over a restricted search space led to the final result: a bilaterally symmetric arrangement of three stars (Figure S2) can easily be translated along its line of mirror symmetry, forming three columns of densely packed stars, which can be extended in the perpendicular direction to fill the plane.

(11) Frantz, D. K.; Linden, A.; Baldrige, K. K.; Siegel, J. S. *J. Am. Chem. Soc.* **2012**, *134*, 1528–1535.

(12) Tsefrikas, V. M.; Scott, L. T. *Chem. Rev.* **2006**, *106*, 4868–4884.

(13) Wu, Y.-T.; Siegel, J. S. *Chem. Rev.* **2006**, *106*, 4843–4867.

(14) Tahara, K.; Balandina, T.; Furukawa, S.; De Feyter, S.; Tobe, Y. *CrystEngComm* **2011**, *13*, 5551–5558.

(15) Jester, S.-S.; Sigmund, E.; Höger, S. *J. Am. Chem. Soc.* **2011**, *133*, 11062–11065.

(16) Tomba, G.; Stengel, M.; Schneider, W.-D.; Baldereschi, A.; De Vita, A. *ACS Nano* **2010**, *4*, 7545–7551.

(17) Ćija, D.; Urgela, J. I.; Papageorgiou, A. C.; Joshi, S.; Auwärter, W.; Seitsonen, A. P.; Klyatskaya, S.; Ruben, M.; Fischer, S.; Vijayaraghavan, S.; Reichert, J.; Barth, J. V. *Proc. Natl. Acad. Sci. U.S.A.* **2013**, *110*, 6678–6681.

(18) Bauert, T.; Merz, L.; Bandera, D.; Parschau, M.; Siegel, J. S.; Ernst, K.-H. *J. Am. Chem. Soc.* **2009**, *131*, 3460–3461.

(19) Guillermet, O.; Niemi, E.; Nagarajan, S.; Bouju, X.; Martrou, D.; Gourdon, A.; Gauthier, S. *Angew. Chem., Int. Ed.* **2009**, *48*, 1970–1973.

(20) Zoppi, L.; Bauert, T.; Siegel, J. S.; Baldrige, K. K.; Ernst, K.-H. *Phys. Chem. Chem. Phys.* **2012**, *14*, 13365–13369.

(21) Parschau, M.; Fasel, R.; Ernst, K.-H.; Gröning, O.; Brandenberger, L.; Schillinger, R.; Greber, T.; Seitsonen, A.; Wu, Y.-T.; Siegel, J. S. *Angew. Chem., Int. Ed.* **2007**, *46*, 8258–8261.

(22) Calmettes, B.; Nagarajan, S.; Gourdon, A.; Abel, M.; Porte L. Coratger, R. *Angew. Chem., Int. Ed.* **2008**, *47*, 6994–6998.

(23) Merz, L.; Parschau, M.; Zoppi, L.; Baldrige, K. K.; Siegel, J. S.; Ernst, K.-H. *Angew. Chem., Int. Ed.* **2009**, *48*, 1966–1969.

(24) Merz, L.; Bauert, T.; Parschau, M.; Koller, G.; Siegel, J. S.; Ernst, K.-H. *Chem. Commun.* **2009**, 5871–5873.

(25) Xiao, W.; Passerone, D.; Ruffieux, P.; Ait-Mansour, K.; Gröning, O.; Tosatti, E.; Siegel, J. S.; Fasel, R. *J. Am. Chem. Soc.* **2008**, *130*, 4767–4771.

(26) Bauert, T.; Baldrige, K. K.; Siegel, J. S.; Ernst, K.-H. *Chem. Commun.* **2011**, *47*, 7995–7997.

(27) Bauert, T.; Zoppi, L.; Koller, G.; Garcia, A.; Baldrige, K. K.; Ernst, K.-H. *J. Phys. Chem. Lett.* **2011**, *2*, 2805–2809.

(28) Schilling, T.; Pronk, S.; Mulder, B.; Frenkel, D. *Phys. Rev. E* **2005**, *71*, 036138/1–6.

(29) Limon Duparcmeur, Y.; Gervois, A.; Troadec, J. P. *J. Phys.: Condens. Matter* **1995**, *7*, 3421–3430.

(30) Sachdev, S.; Nelson, D. R. *Phys. Rev. B* **1985**, *32*, 1480–1502.

(31) Henley, C. L. *Phys. Rev. B* **1986**, *34*, 797–816.

(32) Adsorbate lattices are specified by the transformation matrix notation, here written in $(m_{11}\ m_{12}\ m_{21}\ m_{22})$ format, linking adsorbate lattice vectors (b_1, b_2) to the substrate lattice vectors (a_1, a_2) via $b_1 = m_{11}a_1 + m_{12}a_2$ and $b_2 = m_{21}a_1 + m_{22}a_2$. See Park, R. L.; Madden, H. H. *Surf. Sci.* **1968**, *11*, 188–202.

(33) The M superscript denotes the mirror domain of the 'master matrix'. For matrix selection rules see: Merz, L.; Ernst, K.-H. *Surf. Sci.* **2010**, *604*, 1049–1054.

(34) Zoppi, L.; Garcia, A.; Baldrige, K. K. *J. Phys. Chem. A* **2010**, *114*, 8864–8872.

- (35) Kuperberg, G.; Kuperberg, W. *Discrete Comput. Geom.* **1990**, *5*, 389–397.
- (36) Brańka, A.; Wojciechowski, K. W. *Mol. Phys.* **1993**, *78*, 1513–1526.
- (37) Brańka, A.; Wojciechowski, K. W. *Mol. Phys.* **1991**, *72*, 941–953.
- (38) Brańka, A.; Wojciechowski, K. W. *Phys. Lett.* **1984**, *101A*, 349–352.
- (39) Ernst, K.-H. *Phys. Status Solidi B* **2012**, *249*, 2057–2088.
- (40) Pérez-García, L.; Amabilino, D. B. *Chem. Soc. Rev.* **2007**, *36*, 941–967.
- (41) Buchner, F.; Kellner, I.; Hieringer, W.; Steinrück, H. P.; Marbach, H. *Phys. Chem. Chem. Phys.* **2010**, *12*, 13082–13090.